Signal Processing 108 (2015) 159–166

Contents lists available at ScienceDirect

Signal Processing

journal homepage: www.elsevier.com/locate/sigpro

Joint diagonalization based DOD and DOA estimation for bistatic MIMO radar

Tie-Qi Xia

KEYSIGHT TECHNOLOGIES (Agilent's Electronic Measurement Group is now KEYSIGHT TECHNOLOGIES), TianFu 4th Street, No.116, Chengdu, 610071, PR China

ARTICLE INFO

Article history:
Received 20 February 2014
Received in revised form
5 September 2014
Accepted 9 September 2014
Available online 18 September 2014

Keywords:
Direction of departure
Direction of arrival
Joint diagonalization
Bistatic MIMO radar

ABSTRACT

A novel joint direction of departures (DODs) and direction of arrivals (DOAs) estimator for bistatic multiple-input multiple-output (MIMO) radar via joint diagonalization direction matrices is proposed. The proposed estimator makes use of the MIMO array structure that enables to obtain an extended two-dimensional (2-D) array. Thereby, it may significantly increase the array degrees of freedom (DOFs) to estimate more targets than physical antenna elements. The computation complexity of the proposed method is also shown to be acceptable. Finally, asymptotic performance analysis and numerical experimental results are presented to demonstrate the effectiveness of the proposed method.

1. Introduction

The problem of multiple-input multiple-output (MIMO) arrays has attracted a lot of attention, especially in fields such as radar and communications. MIMO radar uses multiple antennas to simultaneously transmit several orthogonal waveforms and multiple antennas to receive the reflected signals. It has been demonstrated that MIMO antenna systems have more degrees of freedom (DOFs) than those with a single transmit antenna, and thereby dramatically improve the performances of radar and communication systems over conventional phased-arrays [1–9]. Direction of departure (DOD) and direction of arrival (DOA) estimation algorithms have been recently investigated in several papers [2–9]. Yan et al. used a Capon estimator for DOD and DOA estimation, however, its computational complexity is high [2]. Bencheikh et al. worked out combined ESPRIT-root-MUSIC and polynomial root finding techniques to estimate DOD and DOA. They divided the problems into two instances of one-dimensional (1-D) processing. Pair matching techniques are required and additional effort is needed if a pair or more signals have the same 1-D DODs or DOAs [3,4]. Zhang et al. adopted the reduced-dimension MUSIC and the Capon method to reduce the computational complexity for DOD and DOA estimation in MIMO radar [5,6]. Jin et al. proposed joint DOD and DOA estimation algorithm for bistatic MIMO radar based on cross spectral correlation principle. However, no one can handle the case a pair or more of targets have the same 1-D DODs or DOAs. Though the 2-D unitary ESPRIT based DOD and DOA estimation method can handle the case with common 1-D DODs or DOAs [8], their performance might lead to numerical inaccuracies [10].

The model for DOD and DOA estimation is similar to the problem of 2-D DOA estimation. In earlier works, the problem of 2-D DOA has been emphasized in many papers [11–15]. Van der Veen et al. described an algebraically coupled matrix pencil method for determining the 2-D DOAs of a number of plane waves. Zoltowski et al. worked out the 2-D unitary ESPRIT algorithm [12]. Xia et al. proposed several ESPRIT-like methods to handle some existing problems [13–15]. Most methods used for 2-D DOA estimation can be leveraged for DOD and DOA estimation for bistatic MIMO radar. In this paper, a new

E-mail address: yunguihun@163.com

http://dx.doi.org/10.1016/j.sigpro.2014.09.010
0165-1684/

DOD and DOA estimation method based on joint diagonalization (JD) is proposed, which synthesizes the information contained in two DOA matrices and does not have numerical inaccuracies. Furthermore, pair matching techniques are not needed. For comparison, this paper also leverages the 2-D unitary ESPRIT method [12] to MIMO radar, which involves a certain Cayley transformation of the spatial smoothing (SS) matrix to real-valued matrices. It is found that the 2-D unitary ESPRIT method provides a computationally efficient solution scheme but might lead to numerical inaccuracies, particularly when the directions of the targets are close to 0° or 180° [10].

The rest of this paper is organized as follows. In Section 2, a general MIMO radar model is given which will help to perform array processing with increased DOFs. In Section 3, a new JD based DOD and DOA estimation method, called JD direction matrix (JDDM), is presented. In Section 4, asymptotic performance analysis of JDDM based on backward error analysis is provided. In Section 5, the Cramer–Rao Bound for the problem is derived. In Section 6, numerical simulations are presented to illustrate the performance of JDDM algorithm. Conclusions are presented in Section 7.

1.1. Nomenclature

The following list is a summary of some of the notation used in this paper:

M	number of elements of transmit array
N	number of elements of receive array
L	number of codes in one pulse period
D	number of targets
Q	number of transmitted pulses period
$(\cdot)^T$	transpose
$(\cdot)^H$	complex conjugate transpose
$(\cdot)^\dagger$	pseudoinverse
$\otimes$	kronecker matrix product
$\circ$	Schur–Hadamard matrix product
$\mathrm{vec}(\cdot)$	the operator that stacks the columns of a matrix in column vector format
$\mathrm{Im}(\cdot)$	imaginary part of $(\cdot)$

2. Bistatic MIMO radar signal model

Consider an MIMO radar consisting of a transmit antenna array and a receive antenna array. The transmit array has M elements with interelement space d_2, and the receive array has N elements with interelement space d_1. Both arrays are uniform linear arrays (ULA) and all the elements are omnidirectional. It is assumed that the Doppler frequencies have almost no effect on the orthogonality of the signals. Each element of the transmit array transmits orthogonal waveforms $\boldsymbol{s}_i(k)=[s_i(1),s_i(2),\ldots,s_i(L)]^T$ with $i=1,2,\ldots,M$ and $k=1,2,\ldots,L$. For $\boldsymbol{s}_i$ and $\boldsymbol{s}_j$, $i\neq j$, $\boldsymbol{s}_i^H\boldsymbol{s}_j=0$, $\boldsymbol{s}_i^H\boldsymbol{s}_i=|\boldsymbol{s}_i|^2$. These signals are reflected by D targets with directions (α_i,β_i), where α_i is the DOD of the ith target, and β_i is the DOA of the ith target.

In the case of one target and D targets, the received signal vector of one pulse period measured by the receive array can be expressed as

$$\boldsymbol{r}(k)=\gamma\boldsymbol{b}(\beta)\boldsymbol{a}^T(\alpha)\boldsymbol{s}(k)+\boldsymbol{w}(k) \tag{1}$$

and

$$\boldsymbol{r}(k)=\boldsymbol{B}(\beta)\boldsymbol{\kappa}\boldsymbol{A}^T(\alpha)\boldsymbol{S}(k)+\boldsymbol{w}(k), \tag{2}$$

respectively. Where $\boldsymbol{A}=[\boldsymbol{a}_1,\boldsymbol{a}_2,\ldots,\boldsymbol{a}_D]$ and $\boldsymbol{B}=[\boldsymbol{b}_1,\boldsymbol{b}_2,\ldots,\boldsymbol{b}_D]$ are the $M\times D$ transmit and $N\times D$ receive array manifold matrices, respectively. The matrices $\boldsymbol{A}$ and $\boldsymbol{B}$ are unknown and not rank deficient by assumption. Thereby, the mth element of $\boldsymbol{a}_i$ can be written as $e^{j2\pi[d_2(m-1)\cos(\alpha_i)]/\lambda}$, the nth element of $\boldsymbol{b}_i$ can be written as $e^{j2\pi[d_1(n-1)\cos(\beta_i)]/\lambda}$. $\boldsymbol{\gamma}=[\gamma_{11},\gamma_{21},\ldots,\gamma_{D1}]^T$ denotes the reflection coefficients of D targets and $\boldsymbol{\kappa}=diag(\boldsymbol{\gamma})$. $\boldsymbol{S}(k)=[\boldsymbol{s}_1(k),\boldsymbol{s}_2(k),\ldots,\boldsymbol{s}_M(k)]^T$. $\boldsymbol{w}(k)$ is assumed to be temporally and spatially additive white Gaussian noises with mean zero and variance σ_N^2, independent of each other and the signal samples.

For orthogonal transmitted waveforms, the received signal $\boldsymbol{r}(t)$ can be matched by the transmitted waveforms to yield a sufficient statistic matrix as follows [2]:

$$\boldsymbol{Y}=\frac{1}{L}\sum_{k=1}^{L}\boldsymbol{r}(k)\boldsymbol{S}^H(k). \tag{3}$$

When the number of the targets is D and the signals of Q pulses period are transmitted, Eq. (3) can be written as

$$\boldsymbol{X}_\mu=\mathrm{vec}(\boldsymbol{Y}^T)=\boldsymbol{C}(\alpha,\beta)\boldsymbol{F}+\boldsymbol{W}=\boldsymbol{X}_c+\boldsymbol{W}, \tag{4}$$

where $\boldsymbol{C}=[\boldsymbol{c}_1,\boldsymbol{c}_2,\ldots,\boldsymbol{c}_D],\boldsymbol{c}_i=\boldsymbol{b}_i\otimes\boldsymbol{a}_i$. $\boldsymbol{W}$ is complex Gaussian noises with mean zero and variance σ_N^2.

$$\boldsymbol{F}=\begin{bmatrix}\gamma_{11}&\gamma_{12}&\cdots&\gamma_{1Q}\\ \gamma_{21}&\gamma_{22}&\cdots&\gamma_{2Q}\\ \vdots&\vdots&\ddots&\vdots\\ \gamma_{D1}&\gamma_{D2}&\cdots&\gamma_{DQ}\end{bmatrix}=\begin{bmatrix}\boldsymbol{\gamma}_1(v)\\ \boldsymbol{\gamma}_2(v)\\ \vdots\\ \boldsymbol{\gamma}_D(v)\end{bmatrix} \tag{5}$$

where γ_{dv} $(d=1,2,\ldots,D,\quad v=1,2,\ldots,Q)$ is the refection coefficients of the dth target in the vth transmit pulse period. The derivation of (4) is given in Appendix A. Assume $\{\boldsymbol{\gamma}_d(v),\ d=1,2,\ldots,D\}$ is a random sequence that is circularly Gaussian distributed with mean zero and covariance $\boldsymbol{P}=\boldsymbol{F}\boldsymbol{F}^H/Q$.

The auto-covariance matrix of $\boldsymbol{X}_\mu$ is given by $\boldsymbol{R}_{xx}$

$$\begin{aligned}\boldsymbol{R}_{xx}&=\boldsymbol{X}_\mu\boldsymbol{X}_\mu^H/Q\\ &=\boldsymbol{C}(\alpha,\beta)\boldsymbol{P}\boldsymbol{C}^H(\alpha,\beta)+\sigma_N^2\boldsymbol{I}_{MN}\end{aligned} \tag{6}$$

where $\boldsymbol{I}_{MN}$ is an $MN\times MN$ identity matrix.

3. DOD and DOA estimation based on joint diagonalization

The unitary-ESPRIT algorithm involves a certain Cayley transformation of the data to real-valued matrices, which provides a computationally efficient solution scheme but might result in numerical inaccuracies, particularly when the targets are close to 0° or 180°. In this section, a new DOD and DOA estimator based on JD is proposed, which does not have numerical inaccuracies.

3.1. Forming the DOD and DOA matrices

By eigendecomposition,

$$\boldsymbol{R}_{xx} = \boldsymbol{U}_s \boldsymbol{\Lambda}_s \boldsymbol{U}_s^H + \boldsymbol{U}_n \boldsymbol{\Lambda}_n \boldsymbol{U}_n^H. \tag{7}$$

Denote by $\lambda_1, \ldots, \lambda_D$ the D big eigenvalues and $\boldsymbol{h}_1, \ldots, \boldsymbol{h}_D$ the corresponding eigenvectors of $\boldsymbol{R}_{xx}$. The signal subspace of $\boldsymbol{R}_{xx}$ can be written as

$$\boldsymbol{U}_p = \boldsymbol{U}_s \times diag(\lambda_1, \ldots, \lambda_D)^{0.5} = [\boldsymbol{h}_1, \ldots, \boldsymbol{h}_D] \times diag(\lambda_1, \ldots, \lambda_D)^{0.5}$$

where the exponent "0.5" comes from the fact that the target signals are averaged by a power of 2.

Define four selection matrices as,

$$\boldsymbol{J}_1 = \begin{bmatrix} 1 & 0 & \cdots & 0 & 0 \\ 0 & 1 & \cdots & 0 & 0 \\ \vdots & \vdots & \ddots & \vdots & \vdots \\ 0 & 0 & \cdots & 1 & 0 \end{bmatrix} \in \Re^{(M-1)\times M}$$

$$\boldsymbol{J}_2 = \begin{bmatrix} 0 & 1 & 0 & \cdots & 0 \\ 0 & 0 & 1 & \cdots & 0 \\ \vdots & \vdots & \vdots & \ddots & \vdots \\ 0 & 0 & 0 & \cdots & 1 \end{bmatrix} \in \Re^{(M-1)\times M}$$

$$\boldsymbol{J}_3 = \begin{bmatrix} 1 & 0 & \cdots & 0 & 0 \\ 0 & 1 & \cdots & 0 & 0 \\ \vdots & \vdots & \ddots & \vdots & \vdots \\ 0 & 0 & \cdots & 1 & 0 \end{bmatrix} \in \Re^{(N-1)\times N}$$

$$\boldsymbol{J}_4 = \begin{bmatrix} 0 & 1 & 0 & \cdots & 0 \\ 0 & 0 & 1 & \cdots & 0 \\ \vdots & \vdots & \vdots & \ddots & \vdots \\ 0 & 0 & 0 & \cdots & 1 \end{bmatrix} \in \Re^{(N-1)\times N}$$

where, $\boldsymbol{J}_1$ and $\boldsymbol{J}_2$ are the $(M-1)\times M$ selection matrices, $\boldsymbol{J}_1$ and $\boldsymbol{J}_2$ select the first and last $M-1$ components of a $M\times 1$ vector, respectively. $\boldsymbol{J}_3$ and $\boldsymbol{J}_4$ work similarly to $\boldsymbol{J}_1$ and $\boldsymbol{J}_2$, with dimension related to N.

Then the DOD and DOA selection matrices of the algorithm can be expressed as

$$\boldsymbol{K}_{M1} = \boldsymbol{I}_{K1} \otimes \boldsymbol{J}_1, \quad \boldsymbol{K}_{M2} = \boldsymbol{I}_{K1} \otimes \boldsymbol{J}_2, \tag{8}$$

$$\boldsymbol{K}_{N1} = \boldsymbol{J}_3 \otimes \boldsymbol{I}_{K2}, \quad \boldsymbol{K}_{N2} = \boldsymbol{J}_4 \otimes \boldsymbol{I}_{K2}. \tag{9}$$

where both $\boldsymbol{I}_{K1}$ and $\boldsymbol{I}_{K2}$ are identity matrices, with dimension $N\times N$ and $M\times M$, respectively.

Define DOD and DOA matrices as

$$\boldsymbol{G}_{yx} = (\boldsymbol{K}_{M1}\boldsymbol{U}_p)^{\dagger}\boldsymbol{K}_{M2}\boldsymbol{U}_p = \boldsymbol{U}\boldsymbol{\Phi}_1\boldsymbol{U}^H, \tag{10}$$

$$\boldsymbol{G}_{zx} = (\boldsymbol{K}_{N1}\boldsymbol{U}_p)^{\dagger}\boldsymbol{K}_{N2}\boldsymbol{U}_p = \boldsymbol{U}\boldsymbol{\Phi}_2\boldsymbol{U}^H, \tag{11}$$

and

$$\boldsymbol{\Phi}_1 = diag\left[e^{j\frac{2\pi}{\lambda}d_2\cos(\alpha_1)}, \ldots, e^{j\frac{2\pi}{\lambda}d_2\cos(\alpha_D)}\right] = diag[\phi_{11}, \ldots, \phi_{p1}, \ldots, \phi_{q1} \ldots, \phi_{D1}], \quad p\neq q, \quad p,q = 1, \ldots, D, \tag{12}$$

$$\boldsymbol{\Phi}_2 = diag\left[e^{j\frac{2\pi}{\lambda}d_1\cos(\beta_1)}, \ldots, e^{j\frac{2\pi}{\lambda}d_1\cos(\beta_D)}\right] = diag[\phi_{12}, \cdots, \phi_{p2}, \cdots, \phi_{q2} \cdots, \phi_{D2}], \quad p\neq q, \quad p,q = 1, \cdots, D. \tag{13}$$

Let $\tilde{\boldsymbol{G}} = \{\boldsymbol{G}_{yx}, \boldsymbol{G}_{zx}\}$ be a set of two matrices where, for $l = 1, 2$, matrices $\boldsymbol{G}_{yx}$ and $\boldsymbol{G}_{zx}$ are in the form $\boldsymbol{U}\boldsymbol{\Phi}_l\boldsymbol{U}^H$ with $\boldsymbol{U}$ a unitary matrix.

If the targets have common DODs, then Eq. (12) has degenerate eigenvalue spectrum; if the targets have common DOAs, then Eq. (13) has degenerate eigenvalue spectrum. Since we assume two targets should not have common DOD and DOA at the same time, that means the direction pairs (α_i, β_i) are distinct for different targets, then a joint diagonalizer $\boldsymbol{U}$ of $\tilde{\boldsymbol{G}} = \{\boldsymbol{G}_{yx}, \boldsymbol{G}_{zx}\}$ can always be obtained. The joint diagonalizer is of course much weaker than the requirement that there exists a uniquely unitarily diagonalizable matrix in $\tilde{\boldsymbol{G}}$.

Then the DOD and DOA estimation problem reduces to that of determining a unitary $D\times D$ matrix $\boldsymbol{U}$. It can be estimated by using the simultaneous diagonalization method [16,17].

To determine (α_i, β_i) of the ith target, based on (10) and (11), as $\boldsymbol{U}$ is the eigenvector of both $\boldsymbol{G}_{yx}$ and $\boldsymbol{G}_{zx}$, the one-to-one correspondence preserved in the positional correspondence on the diagonals between ϕ_{i1}'s and ϕ_{i2}'s can be obtained. Then $(\widehat{\alpha}_i, \widehat{\beta}_i)$ can be estimated from the following equations:

$$\widehat{\alpha}_i = \cos^{-1}[-\arg(\phi_{i1})\lambda/d_2/2\pi], \tag{14}$$

$$\widehat{\beta}_i = \cos^{-1}[-\arg(\phi_{i2})\lambda/d_1/2\pi], \tag{15}$$

and there's no need for a pair matching operation.

3.2. Implementation of the JDDM algorithm

Based on the previous sections, a new DOD and DOA estimation method (JDDM) is summarized as follows:

1) Estimate the auto-covariance matrix $\boldsymbol{R}_{xx}$.
2) Form $\boldsymbol{G}_{yx}$ and $\boldsymbol{G}_{zx}$.
3) A unitary matrix $\boldsymbol{U}$ is then obtained as joint diagonalizer of the set $\tilde{\boldsymbol{G}} = \{\boldsymbol{G}_{yx}, \boldsymbol{G}_{zx}\}$.
4) Compute (α_i, β_i) $(i = 1, 2, \ldots, D)$.

Note that the maximum number of targets JDDM can handle is minimum $\{M(N-1), N(M-1)\}$. JDDM provides closed-form, automatically paired DOD and DOA angle estimates as long as the angle pairs $(\alpha_i, \beta_i)(i = 1, 2, \ldots, D)$ are distinct. No additional effort is needed if a pair or more targets have common α_i or β_i.

3.3. Computation complexity

In general, the total number of transmitted pulses Q is much greater than the number of elements, i.e., $Q \gg MN$. Forming the sample covariance matrix requires on the order of $(MN)^2Q$, eigendecompositions of a $MN\times MN$ dimensional matrix requires on the order of $O((MN)^3)$ [13]. Joint diagonalizer of the set $\tilde{\boldsymbol{G}}$ (two $D\times D$ matrices) requires in the order of $2O(D^3)$ [14,15]. The main computation flops of JDDM algorithm is about $((MN)^2Q + O((MN)^3) + 2O(D^3))$.

4. Asymptotic performance analysis of JDDM

In this section, the asymptotic performance of the JDDM estimator is derived. The derivation in this paper is along the lines of the first-order analysis done by Rao [18] and the backward error analysis done by Li [19].

4.1. Perturbation of DOD and DOA

Subspace decomposition can also be performed using SVD of $\boldsymbol{X}_c$ as follows:

$$\boldsymbol{X}_c = \boldsymbol{U}_c\boldsymbol{\Sigma}\boldsymbol{V}_c^H = (\boldsymbol{U}_s \quad \boldsymbol{U}_n)\begin{pmatrix}\boldsymbol{\Sigma}_s & 0\\ 0 & 0\end{pmatrix}\begin{pmatrix}\boldsymbol{V}_s^H\\ \boldsymbol{V}_n^H\end{pmatrix}$$

In JDDM, joint diagonalization is applied to $\tilde{\boldsymbol{G}}$ to obtain $\boldsymbol{U}=[\boldsymbol{f}_1,\boldsymbol{f}_2,\ldots,\boldsymbol{f}_D]$ and its associated eigenvalue matrices $\boldsymbol{\Phi}_1$ and $\boldsymbol{\Phi}_2$. For $\boldsymbol{G}_{yx}$ and $\boldsymbol{G}_{zx}$, there are $\phi_{i1}=\boldsymbol{f}_i^H\boldsymbol{G}_{yx}\boldsymbol{f}_i$ and $\phi_{i2}=\boldsymbol{f}_i^H\boldsymbol{G}_{zx}\boldsymbol{f}_i$, following the first-order approximation principles [18,19], I have

$$\delta\phi_{i1} \approx \boldsymbol{f}_i^H(\boldsymbol{K}_{M1}\boldsymbol{U}_x)^\dagger(\boldsymbol{K}_{M2}-\phi_{i1}\boldsymbol{K}_{M1})\delta\boldsymbol{U}_x\boldsymbol{f}_i, \tag{16}$$

$$\delta\phi_{i2} \approx \boldsymbol{f}_i^H(\boldsymbol{K}_{N1}\boldsymbol{U}_x)^\dagger(\boldsymbol{K}_{N2}-\phi_{i2}\boldsymbol{K}_{N1})\delta\boldsymbol{U}_x\boldsymbol{f}_i, \tag{17}$$

where

$$\boldsymbol{U}_x=\boldsymbol{U}_s\boldsymbol{\Sigma}_s,$$

$$\delta\boldsymbol{U}_s=\boldsymbol{U}_n\boldsymbol{U}_n^H\boldsymbol{W}\boldsymbol{V}_s\boldsymbol{\Sigma}_s^{-1},$$

$$\delta\boldsymbol{U}_x=\delta\boldsymbol{U}_s\boldsymbol{\Sigma}_s=\boldsymbol{U}_n\boldsymbol{U}_n^H\boldsymbol{W}\boldsymbol{V}_s.$$

For MIMO DOD and DOA estimation, the quantities of interest are α_i and β_i, which are related to ϕ_{i1} and ϕ_{i2} as demonstrated by (18) and (19).

Using a first-order Taylor series expansion [18,19], $\delta\alpha_i$ and $\delta\beta_i$ can be expressed as,

$$\delta\alpha_i = C_\alpha \mathrm{Im}\left(\frac{\delta\phi_{i1}}{\phi_{i1}}\right), \tag{18}$$

$$\delta\beta_i = C_\beta \mathrm{Im}\left(\frac{\delta\phi_{i2}}{\phi_{i2}}\right), \tag{19}$$

where $C_\alpha=\lambda/(2\pi d_2\ \sin\ \alpha_i)$, $C_\beta=\lambda/(2\pi d_1\ \sin\ \beta_i)$. The perturbation of the ith DOD and DOA are

$$\delta\alpha_i = C_\alpha \mathrm{Im}\left(\frac{\boldsymbol{f}_i^H(\boldsymbol{K}_{M1}\boldsymbol{U}_x)^\dagger(\boldsymbol{K}_{M2}\boldsymbol{U}_n-\phi_{i1}\boldsymbol{K}_{M1}\boldsymbol{U}_n)\boldsymbol{U}_n^H\boldsymbol{W}\boldsymbol{V}_s\boldsymbol{f}_i}{\phi_{i1}}\right) \tag{20}$$

and

$$\delta\beta_i = C_\beta \mathrm{Im}\left(\frac{\boldsymbol{f}_i^H(\boldsymbol{K}_{N1}\boldsymbol{U}_x)^\dagger(\boldsymbol{K}_{N2}\boldsymbol{U}_n-\phi_{i2}\boldsymbol{K}_{N1}\boldsymbol{U}_n)\boldsymbol{U}_n^H\boldsymbol{W}\boldsymbol{V}_s\boldsymbol{f}_i}{\phi_{i2}}\right). \tag{21}$$

4.2. Statistical performance

As seen in (20) and (21), the perturbation of direction is linear in the noise, so to first order, the predicted bias of estimated direction is zero. This follows from the fact that the noise is independent identically distributed both spatially and temporally with mean zero.

The error-variance of estimated DOD and DOA are

$$\mathrm{var}(\delta\alpha_i)=\frac{1}{2}C_\alpha^2\mathrm{var}\left(\frac{\delta\phi_{i1}}{\phi_{i1}}\right)=\frac{C_\alpha^2\sigma_N^2}{2}\frac{\boldsymbol{\xi}_1^H\boldsymbol{\xi}_1}{|\phi_{i1}|^2} \tag{22}$$

where

$$\boldsymbol{\xi}_1^H=\boldsymbol{f}_i^H(\boldsymbol{K}_{M1}\boldsymbol{U}_x)^\dagger(\boldsymbol{K}_{M2}\boldsymbol{U}_n-\phi_{i1}\boldsymbol{K}_{M1}\boldsymbol{U}_n),$$

and

$$\mathrm{var}(\delta\beta_i)=\frac{1}{2}C_\beta^2\mathrm{var}\left(\frac{\delta\phi_{i1}}{\phi_{i1}}\right)=\frac{C_\beta^2\sigma_N^2}{2}\frac{\boldsymbol{\xi}_2^H\boldsymbol{\xi}_2}{|\phi_{i2}|^2}. \tag{23}$$

where

$$\boldsymbol{\xi}_2^H=\boldsymbol{f}_i^H(\boldsymbol{K}_{N1}\boldsymbol{U}_x)^\dagger(\boldsymbol{K}_{N2}\boldsymbol{U}_n-\phi_{i2}\boldsymbol{K}_{N1}\boldsymbol{U}_n).$$

Notice that $|\phi_{i1}|^2=1$ and $|\phi_{i2}|^2=1$ for the noise free case, I have

$$\mathrm{var}(\delta\alpha_i)=\frac{C_\alpha^2\sigma_N^2}{2}\left\|\boldsymbol{f}_i^H(\boldsymbol{K}_{M1}\boldsymbol{U}_x)^\dagger(\boldsymbol{K}_{M2}\boldsymbol{U}_n-\phi_{i1}\boldsymbol{K}_{M1}\boldsymbol{U}_n)\right\|^2 \tag{24}$$

and

$$\mathrm{var}(\delta\beta_i)=\frac{C_\beta^2\sigma_N^2}{2}\left\|\boldsymbol{f}_i^H(\boldsymbol{K}_{N1}\boldsymbol{U}_x)^\dagger(\boldsymbol{K}_{N2}\boldsymbol{U}_n-\phi_{i2}\boldsymbol{K}_{N1}\boldsymbol{U}_n)\right\|^2. \tag{25}$$

Note that the eigendecomposition result $\boldsymbol{U}_p$ of noise free $\boldsymbol{R}_{xx}$ in (7) can also be used for asymptotic calculation, then Eqs. (24) and (25) can be written as,

$$\mathrm{var}(\delta\alpha_i)=\frac{C_\alpha^2\sigma_N^2}{2Q}\left\|\boldsymbol{f}_i^H(\boldsymbol{K}_{M1}\boldsymbol{U}_p)^\dagger(\boldsymbol{K}_{M2}\boldsymbol{U}_n-\phi_{i1}\boldsymbol{K}_{M1}\boldsymbol{U}_n)\right\|^2 \tag{26}$$

and

$$\mathrm{var}(\delta\beta_i)=\frac{C_\beta^2\sigma_N^2}{2Q}\left\|\boldsymbol{f}_i^H(\boldsymbol{K}_{N1}\boldsymbol{U}_p)^\dagger(\boldsymbol{K}_{N2}\boldsymbol{U}_n-\phi_{i2}\boldsymbol{K}_{N1}\boldsymbol{U}_n)\right\|^2 \tag{27}$$

If α_i and β_i are given in degrees instead of radians, a corresponding scale should be considered [20].

Finally, the DOD and DOA asymptotic performance of the JDDM estimator is derived as:

$$\mathrm{var}(\delta\alpha_i,\delta\beta_i)=\mathrm{var}(\delta\alpha_i)+\mathrm{var}(\delta\beta_i). \tag{28}$$

5. Cramer–Rao bound

In this section, the stochastic Cramer–Rao bound (CRB) for the problem of DOD and DOA using MIMO is briefly derived. The result is a generalization of a similar result in [13,21].

Using (4), the signal model can be rewritten as

$$\boldsymbol{X}_\mu=\boldsymbol{C}(\alpha,\beta)\boldsymbol{F}+\boldsymbol{W}. \tag{29}$$

Let me introduce the following $2D\times 1$ vector

$$\boldsymbol{\eta}=[\boldsymbol{\alpha}^T\boldsymbol{\beta}^T]^T=[\alpha_1,\ldots,\alpha_D,\beta_1,\ldots,\beta_D]^T. \tag{30}$$

The unknown parameters of the problem include the elements of the vector $\boldsymbol{\eta}$, the noise variance σ_N^2, and the parameters of the target covariance matrix ($\boldsymbol{P}_{dd}$) $(1\le d\le D)$ and $\{\mathrm{Re}[\boldsymbol{P}_{dl}],\quad \mathrm{Im}[\boldsymbol{P}_{dl}];\quad d>l\}(1\le d,\quad l\le D)$.

Concentrating the problem with respect to the parameters of the covariance matrix and the noise variance, there is the following equation for the entries of the $2D\times 2D$

CRB matrix

$$[\mathrm{CRB}^{-1}(\boldsymbol{\eta})]_{kl}=\frac{2Q}{\sigma_N^2}\mathrm{Re}\left\{\boldsymbol{U}_q\frac{\partial \boldsymbol{C}^H}{\partial \eta_l}\boldsymbol{S}_{\boldsymbol{C}}^{\perp}\frac{\partial \boldsymbol{C}}{\partial \eta_k}\right\} \tag{31}$$

where

$$\boldsymbol{U}_q=\boldsymbol{P}(\boldsymbol{C}^H\boldsymbol{C}\boldsymbol{P}+\sigma_N^2\boldsymbol{I})^{-1}\boldsymbol{C}^H\boldsymbol{C}\boldsymbol{P} \tag{32}$$

is the $D\times D$ matrix, and

$$\boldsymbol{S}_{\boldsymbol{C}}^{\perp}=\boldsymbol{I}-\boldsymbol{C}(\boldsymbol{C}^H\boldsymbol{C})^{-1}\boldsymbol{C}^H \tag{33}$$

is the $2M\times 2M$ orthogonal projection matrix.

Following the steps in [21], after complex derivations using (31), the CRB matrix can be expressed in a compact form as

$$\mathrm{CRB}(\boldsymbol{\eta})=\frac{\sigma_N^2}{2Q}\mathrm{Re}\left\{(1\cdot 1^T\otimes \boldsymbol{U}_q)\circ(\boldsymbol{D}^H\boldsymbol{S}_{\boldsymbol{C}}^{\perp}\boldsymbol{D})^T\right\}^{-1} \tag{34}$$

where 1 is a 2×1 vector of ones. Here, the matrix $\boldsymbol{D}$ is defined as

$$\boldsymbol{D}=[\boldsymbol{D}_\alpha,\boldsymbol{D}_\beta] \tag{35}$$

where

$$\boldsymbol{D}_\alpha=\left[\frac{\partial \boldsymbol{c}(\alpha_1,\beta_1)}{\partial\alpha_1},\ldots,\frac{\partial \boldsymbol{c}(\alpha_D,\beta_D)}{\partial\alpha_D}\right],$$
$$\boldsymbol{D}_\beta=\left[\frac{\partial \boldsymbol{c}(\alpha_1,\beta_1)}{\partial\beta_1},\ldots,\frac{\partial \boldsymbol{c}(\alpha_D,\beta_D)}{\partial\beta_D}\right].$$

6. Computer simulations

Simulations are carried out to illustrate the performance of the proposed JDDM algorithm. Results are also compared with those of the leveraged Unitary ESPRIT algorithm [12]. In the simulations, suppose $M=4$, $N=4$. For easy comparison, performance analysis and CRB results are also given. The performances of the estimators are obtained from 500 Monte-Carlo simulations, by calculating the RMSEs of the direction estimates. The RMSE of $s_i(t)$ $(i=1\text{–}4)$ is defined as Fig. 1

$$\mathrm{RMSE}_i=\sqrt{E[(\hat{\alpha}_i-\alpha_i)^2+(\hat{\beta}_i-\beta_i)^2]}.$$

Example 1. In the first example, the scenario is consisted of four uncorrelated narrowband target signals with (DOD, DOA) pairs $(20^\circ,20^\circ)$,$(20^\circ,40^\circ)$, $(40^\circ,20^\circ)$ and $(40^\circ,40^\circ)$. $s_1(t)$ and $s_2(t)$ have common α_1, $s_3(t)$ and $s_4(t)$ have common α_2, $s_1(t)$ and $s_3(t)$ have common β_1, $s_2(t)$ and $s_4(t)$ have common β_2. The number of transmitted pulses is 300. Figs. 2–5 show the RMSEs in degrees of the estimates of the four targets when signal to noise ratio (SNR) is varied from -5 to 15 dB. The performance of JDDM algorithm is observed to outperform unitary ESPRIT algorithm at low SNRs. The performance of unitary ESPRIT is heavily affected by the direction (DOD or DOA) closer to 0° particularly at low SNRs.

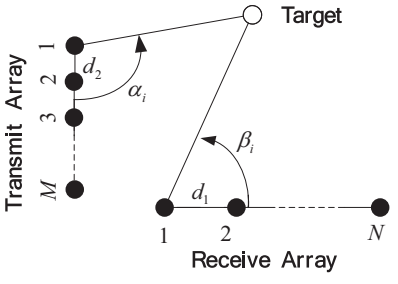

Fig. 1. Bistatic MIMO radar scenario.

Example 2. In second example, the performance change versus the number of transmitted pulses is simulated. The same targets scenario as Example 1 is used and the SNR is set to 5 dB. The number of transmitted pulses is varied from 50 to 1000. Figs. 6–9 show that the performance of JDDM algorithm outperforms unitary ESPRIT algorithm with small number of transmitted pulses. The performance of unitary ESPRIT is heavily affected by the direction (DOD or DOA) closer to 0° particularly when the number of transmitted pulses is small.

Example 3. In this example, the performance of JDDM versus target locations is examined. Assume there are

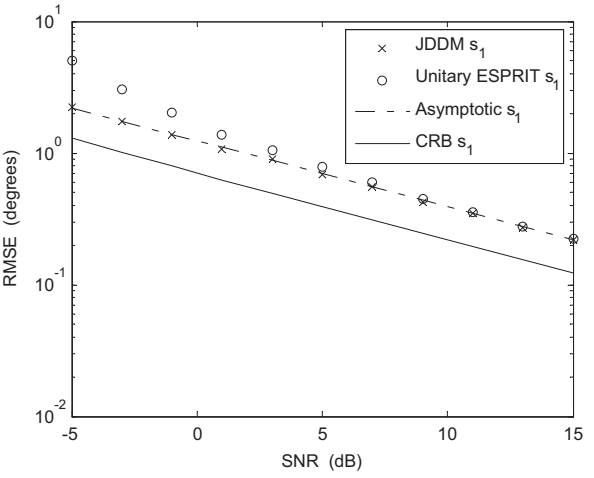

Fig. 2. RMSE of target 1 versus SNR.

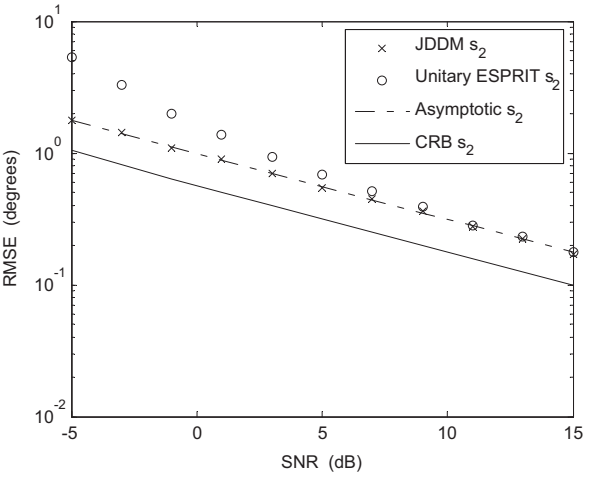

Fig. 3. RMSE of target 2 versus SNR.

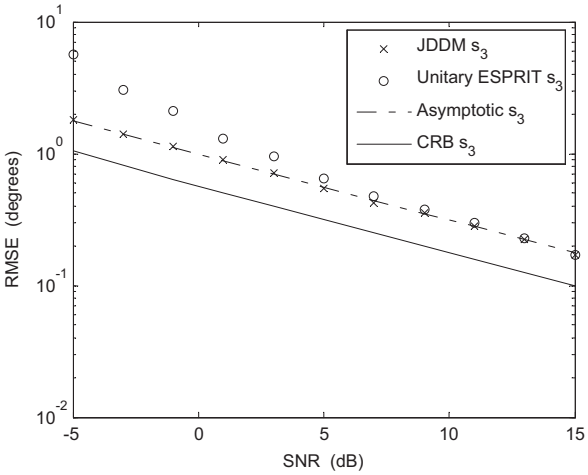

Fig. 4. RMSE of target 3 versus SNR.

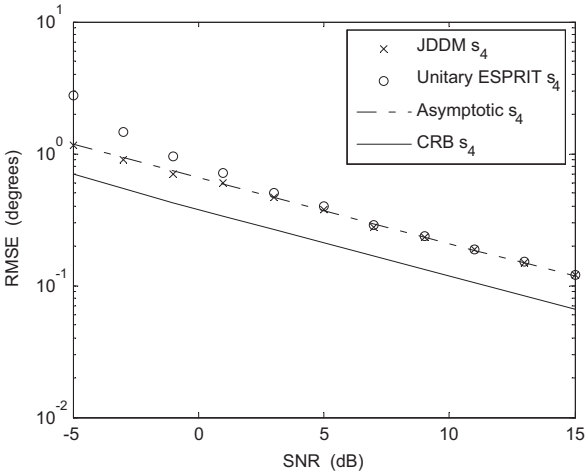

Fig. 5. RMSE of target 4 versus SNR.

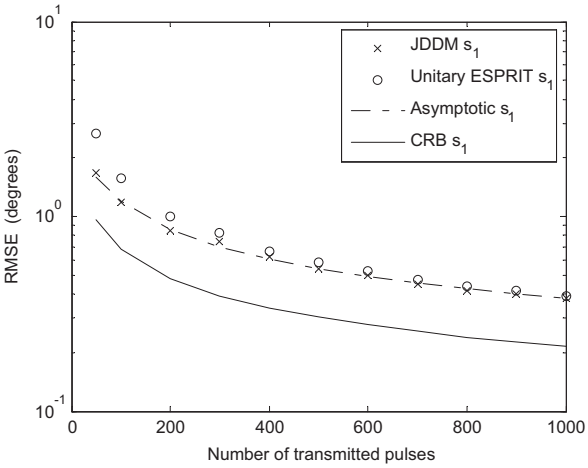

Fig. 6. RMSE of target 1 versus number of transmitted pulses.

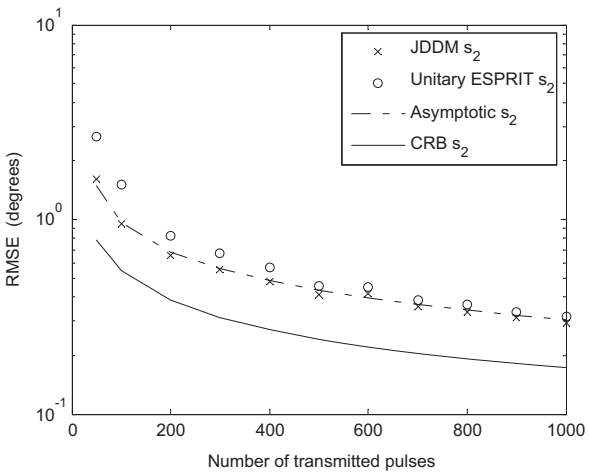

Fig. 7. RMSE of target 2 versus number of transmitted pulses.

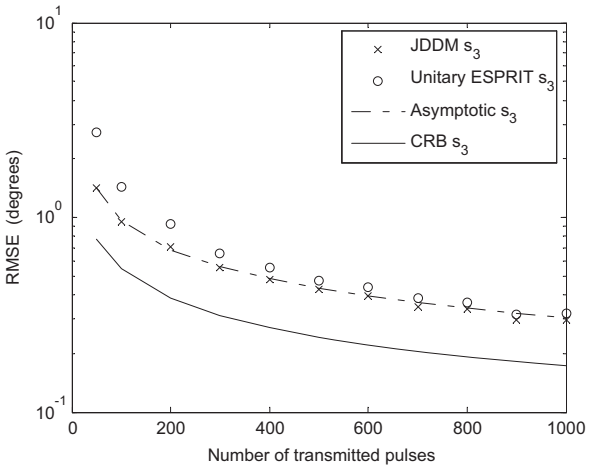

Fig. 8. RMSE of target 3 versus number of transmitted pulses.

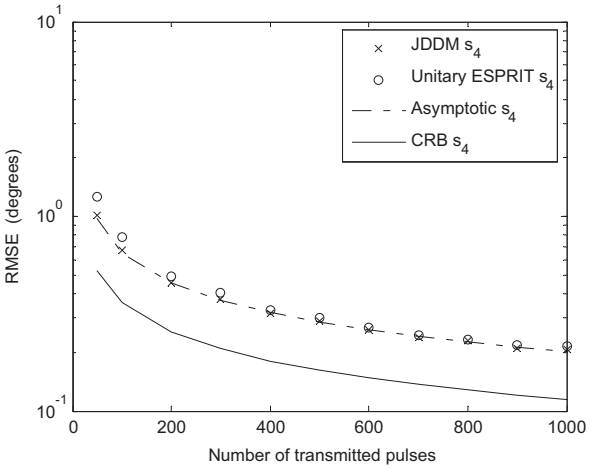

Fig. 9. RMSE of target 4 versus number of transmitted pulses.

several groups of uncorrelated narrowband targets. The directions in each target group are $((10+\Delta)^\circ,(10+\Delta)^\circ)$, $((10+\Delta)^\circ,(30+\Delta)^\circ)$, $((30+\Delta)^\circ,(10+\Delta)^\circ)$ and $((30+\Delta)^\circ,(30+\Delta)^\circ)$. The number of transmitted pulses is 300 and SNR is 10 dB. The RMSEs of the estimates of the targets are shown in Figs. 10–13 when Δ is changed from 0° to 30°.

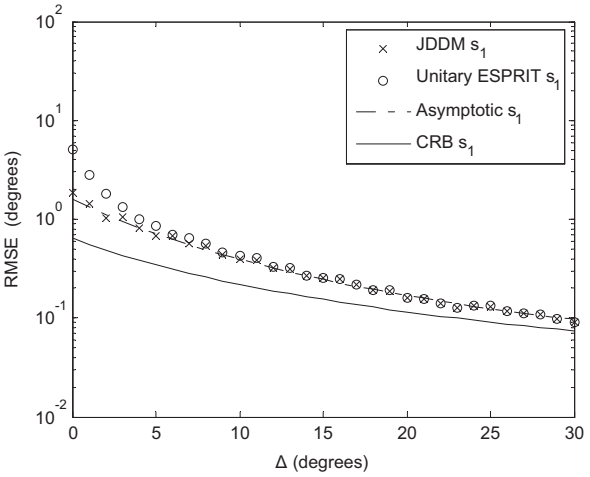

Fig. 10. RMSE of target 1 versus Δ.

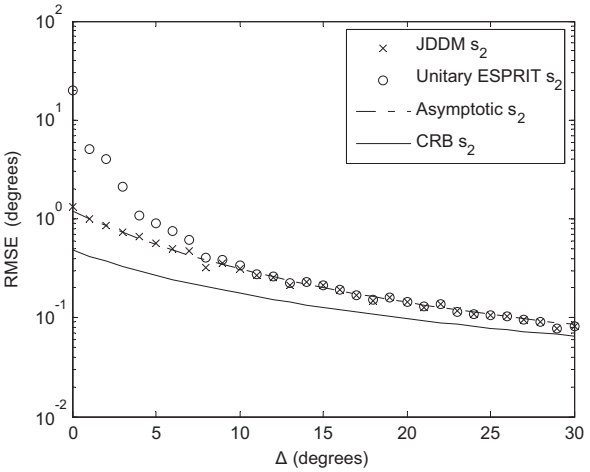

Fig. 11. RMSE of target 2 versus Δ.

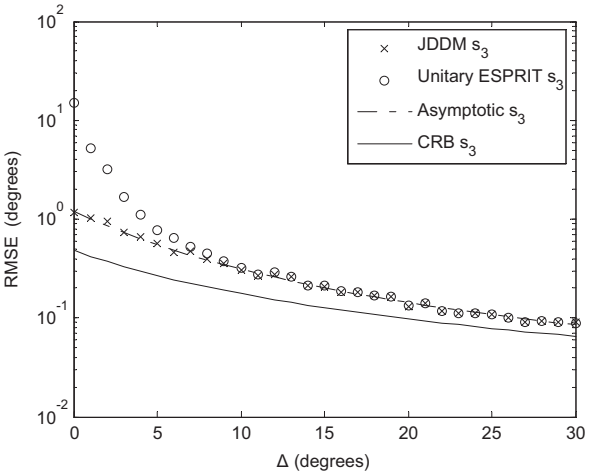

Fig. 12. RMSE of target 3 versus Δ.

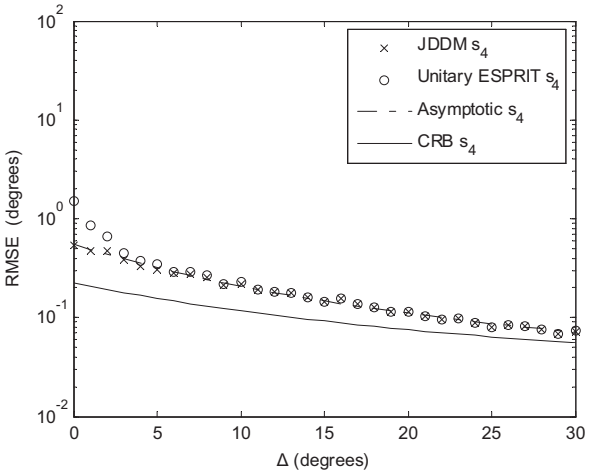

Fig. 13. RMSE of target 4 versus Δ.

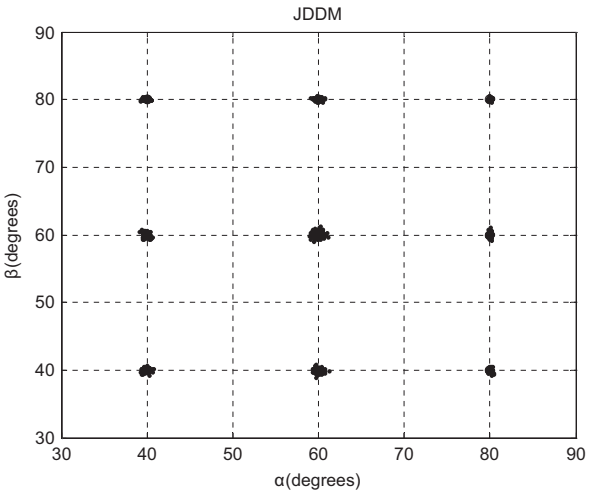

Fig. 14. Scatter plot the JDDM method.

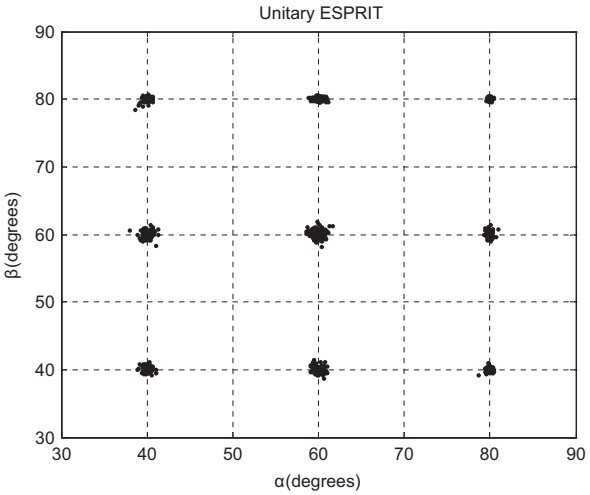

Fig. 15. Scatter plot of the Unitary ESPRIT method.

The performance of JDDM algorithm is observed to be better than unitary ESPRIT algorithm when Δ is small.

Example 4. In this example, assume that 9 targets with DOD and DOA pairs are indicated by the "circle" in Figs. 14 and 15. The number of transmitted pulses is 1000 and SNR is 10 dB. To obtain a measure of statistical repeatability, 100 Monte-Carlo simulations are executed. Figs. 14 and 15 show that both methods can estimate more targets than the physical elements. Both methods can estimate target signals with common DODs and DOAs. However, the estimates of JDDM are relatively more concentrated than those of unitary ESPRIT.

7. Conclusions

In this paper, a new JD based DOD and DOA estimation method for MIMO radar is proposed. It avoids the numerical inaccuracies caused by unitary transformation and pair matching techniques are not needed. Following the principle of backward error analysis, method for the DOD and DOA first-order performance analysis is presented. Numerical examples show the excellent performance of the proposed method.

Appendix A

When the number of the targets is D and one pulse period is transmitted, substitution of (2) into (3), the independent sufficient statistic vector can be expressed as

$$\begin{aligned}\boldsymbol{Y} &= \frac{1}{L}\sum_{k=1}^{L}[\boldsymbol{B}(\beta)\boldsymbol{\kappa}\boldsymbol{A}^T(\alpha)\boldsymbol{S}(k)+\boldsymbol{w}(k)]\boldsymbol{S}^H(k)\\ &= \boldsymbol{B}(\beta)\boldsymbol{\kappa}\boldsymbol{A}^T(\alpha)\frac{1}{L}\sum_{k=1}^{L}[\boldsymbol{S}(k)\boldsymbol{S}^H(k)]+\frac{1}{L}\sum_{k=1}^{L}[\boldsymbol{w}(k)\boldsymbol{S}^H(k)]\\ &= \boldsymbol{B}(\beta)\boldsymbol{\kappa}\boldsymbol{A}^T(\alpha)\boldsymbol{R}_s+\frac{1}{L}\sum_{k=1}^{L}[\boldsymbol{w}(k)\boldsymbol{S}^H(k)] \qquad (A.1)\end{aligned}$$

where $\boldsymbol{R}_s=(1/L)\sum_{k=1}^{L}[\boldsymbol{S}(k)\boldsymbol{S}^H(k)]$, and $\boldsymbol{R}_s$ is the identity matrix when transmitted signals are orthogonal.

$$\begin{aligned}\boldsymbol{X}_\mu &= \mathrm{vec}(\boldsymbol{Y}^T)\\ &= \mathrm{vec}\left\{[\boldsymbol{B}(\beta)\boldsymbol{\kappa}\boldsymbol{A}^T(\alpha)]^T\right\}+\mathrm{vec}\left\{\left[\frac{1}{L}\sum_{k=1}^{L}[\boldsymbol{w}(k)\boldsymbol{S}^H(k)]\right]^T\right\}\end{aligned} \qquad (A.2)$$

Notice that

$$\begin{aligned}\mathrm{vec}\left\{[\boldsymbol{B}(\beta)\boldsymbol{\kappa}\boldsymbol{A}^T(\alpha)]^T\right\} &= \mathrm{vec}\left\{\boldsymbol{A}(\alpha)\boldsymbol{\kappa}^T\boldsymbol{B}^T(\beta)\right\}\\ &= [\boldsymbol{B}(\beta)\otimes\boldsymbol{A}(\alpha)]\mathrm{vec}\{\boldsymbol{\kappa}^T\}. \qquad (A.3)\end{aligned}$$

As $\boldsymbol{\kappa}$ is a diagonal matrix, many entries of $\mathrm{vec}\{\boldsymbol{\kappa}^T\}$ are zeroes, (A.3) can be simplified as

$$[\boldsymbol{B}(\beta)\otimes\boldsymbol{A}(\alpha)]\mathrm{vec}\{\boldsymbol{\kappa}^T\}=\boldsymbol{C}(\alpha,\beta)\boldsymbol{F} \qquad (A.4)$$

where $\boldsymbol{C}=[\boldsymbol{c}_1,\boldsymbol{c}_2,\ldots,\boldsymbol{c}_D]$, $\boldsymbol{c}_i=\boldsymbol{b}_i\otimes\boldsymbol{a}_i$, $\mathbf{F}=\boldsymbol{\gamma}$. Similarly,

$$\boldsymbol{W}=\mathrm{vec}\left\{\left[\frac{1}{L}\sum_{k=1}^{L}[\boldsymbol{w}(k)\boldsymbol{S}^H(k)]\right]^T\right\}. \qquad (A.5)$$

When the signals of Q pulses period are transmitted, $\boldsymbol{F}$ can be expressed as Eq. (5).

Appendix B. Supporting information

Supplementary data associated with this article can be found in the online version at http://dx.doi.org/10.1016/j.sigpro.2014.09.010.

References

[1] E. Fishler, A. Haimovich, R.S. Blum, L.J. Cimini, D. Chizhik, R.A. Valenzuela, Spatial diversity in radars-models and detection performance, IEEE Trans. Signal Process. 54 (2006) 823–838.
[2] H. Yan, J. Li, G. Liao, Multitarget identification and localization using bistatic MIMO radar systems, EURASIP J. Adv. Signal Process. (2008) 8. (Article ID283483).
[3] M.L. Bencheikh, Y. Wang, Combined ESPRIT-rootMUSIC for DOA-DOD Estimation in polarimetric bistatic MIMO radar, Prog. Electromagn. Res. Lett. 22 (2011) 109–117.
[4] M.L. Bencheikh, Y. Wang, H. He, Polynomial root finding technique for joint DOA DOD estimation in bistatic MIMO radar, Signal Process. 90 (2010) 2723–2730.
[5] X. Zhang, L. Xu, L. Xu, D. Xu, Direction of departure (DOD) and direction of arrival (DOA) estimation in MIMO radar with reduced-dimension MUSIC, IEEE Commun. Lett. 14 (2010) 1161–1163.
[6] X. Zhang, D. Xu, Angle estimation in MIMO radar using reduced-dimension Capon, Electron. Lett. 46 (2010) 860–861.
[7] M. Jin, G. Liao, J. Li, Joint DOD and DOA estimation for bistatic MIMO radar, Signal Process. 89 (2009) 244–251.
[8] H.L. Miao, M. Juntti, K. Yu, 2-D 2-D Unitary ESPRIT Based Joint AOA and AOD Estimation for MIMO System, in: Proceedings of the 2006 IEEE 17th International Symposium on Personal, Indoor and Mobile Radio Communications, vol. 9, no. 11–14, 2006, pp. 1–5.
[9] X. Liu, G. Liao, Joint DOD and DOA estimation using real polynomial rooting in bistatic MIMO radar, in: Proceedings of the 2010 International Conference on Multimedia Technology (ICMT), vol. 10, no. 29–31, 2010, pp. 1–4.
[10] A.N. Lemma, A.J. Van der Veen, E.F. Deprettere, Analysis of joint angle-frequency estimation using ESPRIT, IEEE Trans. Signal Process. 51 (2003) 1264–1282.
[11] A.J. Van der Veen, P.B. Ober, E.F. Deprettere, Azimuth and elevation computation in high resolution DOA estimation, IEEE Trans. Signal Process. 40 (1992) 1828–2832.
[12] M.D. Zoltowski, M. Haardt, C.P. Mathews, Closed-form 2-D angle estimation with rectangular arrays in element space or beamspace via unitary ESPRIT, IEEE Trans. Signal Process. 44 (1996) 316–322.
[13] T.Q. Xia, Y. Zheng, Q. Wan, X. Wang, Decoupled estimation of 2-D angles of arrival using two parallel uniform linear arrays, IEEE Trans. Antennas Propag. 55 (2007) 2627–2632.
[14] T.Q. Xia, X.G. Wang, Y. Zheng, Q. Wan, Joint diagonalization DOA matrix method, Sci. China Ser. F: Inf. 51 (2008) 1340–1348.
[15] T.Q. Xia, Q. Wan, X.G. Wang, Y. Zheng, 2-D DOAs estimation in impulsive noise environments using joint diagonalization fractional lower-order spatio-temporal matrices, Sci. China Ser. F: Inf. 51 (2008) 1585–1593.
[16] A. Belouchrani, K. Abed Meraim, J.F. Cardoso, E. Moulines, A blind source separation technique using second-order statistics, IEEE Trans. Signal Process. 45 (1997) 434–444.
[17] J.F. Cardoso, A. Souloumiac, Jacobi angles for simultaneous diagonalization, SIAM J. Matrix Anal. Appl. 17 (1996) 161–164.
[18] B.D. Rao, K.V.S. Hari, Performance analysis of ESPRIT and TAM in determining the direction of arrival of plane waves in noise, IEEE Trans. Acoust. Speech Signal Process. 37 (1989) 1990–1995.
[19] F. Li, R.J. Vaccaro, D.W. Tufts, Performance analysis of the state-space realization (TAM) and ESPRIT algorithms for DOA estimation, IEEE Trans. Antennas Propag. 39 (1991) 418–423.
[20] N. Yuen, B. Friedlander, Asymptotic performance analysis of ESPRIT, higher order ESPRIT, and virtual ESPRIT algorithms, IEEE Trans. Signal Process. 44 (1996) 2537–2550.
[21] A. Nehorai, E. Paldi, Vector-sensor array processing for electromagnetic source localization, IEEE Trans. Signal Process. 42 (1994) 376–398.